

Acid Modified Activated Carbon Derived from Chestnut Oak Shells for Adsorption and Removal of Methylene Blue from Aqueous Solution

F. Shirzadi¹, B. Ebrahimi¹, A. Roostaie^{*2}, S. Mohammadiazar^{**1}

¹ Department of Chemistry, Sanandaj Branch, Islamic Azad University, P.O. Box: 618, Sanandaj, Iran.

² Police Technology & Equipment Department, Policing Sciences & Social Studies Institute, P.O. Box: 168, Tehran, Iran.

ARTICLE INFO

Article history:

Received: 20 May 2022

Final Revised: 04 Novr 2022

Accepted: 06 Nov 2022

Available online: 31 Dec 2022

Keywords:

Dye removal

Activated carbon

Chestnut shell

Adsorption

Acid modified

Methylene blue

ABSTRACT

In this study, an acid-modified-activated carbon was prepared from the chestnut oak shell as raw material. Carbonization followed by modifying with hydrochloric acid /nitric acid (HCl/HNO₃) was done. Then the modified adsorbent was used to remove methylene blue from aqueous solutions. Different techniques, including scanning electron microscopy (SEM), Brunauer-Emmett-Teller (BET) analysis, and Fourier transform infrared spectroscopy (FTIR), were used for the characterization of the adsorbent. The effects of some experimental parameters, such as pH, adsorbent dosage, contact time, and initial methylene blue concentration, on the removal efficiency were optimized. The optimized parameters were found to be pH, 7, adsorbent dosage, 0.1 g, contact time, 20 min, and initial dye concentration, 50-400 mg L⁻¹. Different Adsorption kinetics and equilibrium were well described by the pseudo-second-order ($R^2 = 0.9996$) and the Freundlich model compared to the other investigated models. The maximum adsorption capacity of methylene blue was found to be 406.21 mg g⁻¹ which was superior or comparable to other reported adsorbents. The results indicated that the prepared acid-modified adsorbent is efficient for methylene blue removal in wastewater treatments. Prog. Color Colorants Coat. 16 (2023), 139-152© Institute for Color Science and Technology.

1. Introduction

Health and safety of water resources have a crucial role in human health. However, with the rapid development in industrialization and urbanization, the discharge of industrial effluents containing toxic organic and inorganic contaminants into the water bodies have been increased [1]. Dyes as an important category of organic pollutants found in various industrial effluents such as textile, paint, plastic, cosmetics, leather, and food [2, 3]. These substances can cause adverse effects on human health and the environment since they have high stability, non-degradability, and potential mutagenic and biotoxicity effects [4, 5]. Therefore, developing a highly

efficient method to remove organic dyes from aqueous media before being discharged to the environment is urgently needed to reduce their negative effect. Among the developed methods for dye removal, adsorption has been considered as a promising technique with the advantages of easy and simple operation, low consumption of energy, cost-effectiveness and environmental friendliness [6, 7]. Adsorbent materials related structurally to carbon such as activated carbon, carbon nanotube and graphene are a number of manufactured substances prescribed to assist the removal of pollutants in contaminated water media. Activated carbon (AC) is one of the most used adsorbents in

*Corresponding author: * ali.roostaie1@gmail.com

** mohammadiazar@iausdj.ac.ir

adsorption processes due to their availability, high surface areas, porous structures, and good chemical and physical stability [8]. However, the high cost of commercially available activated carbons, mainly due to the use of expensive precursors (such as lignite and coal), has limited their application, and thus great efforts have been devoted to finding low cost, renewable and economically feasible sources to produce more effective ACs [9]. Many natural, industrial or agricultural wastes such as banana peels [10], pistachio wood [8], Coconut shell [11], long-root *Eichhornia crassipes* [12], *Ziziphus lotus* stones [13], peanut shell [14], coffee waste [15], date stone [16], tire waste [17, 18], *etc.* have been reported as precursors to prepared ACs which are then applied for removing a wide kinds of contaminants.

In adsorption processes, the chemical functional groups of ACs play a significant role in their treatment efficiencies. For example, acidic groups increase the removal efficiency of cationic species, while basic functional groups can increase the adsorption of anionic species from aqueous solutions [19]. The surface acidity and type and quantity of functional groups presented in the surface of pristine ACs hardly provide requirements for adsorbing contaminants in water samples [20]. Therefore, it is necessary to modify activated carbons using physical or chemical methods to improve their selectivity during the adsorption process. For this purpose, activated carbons are prepared by a two-stage process including a primary carbonization step and second activation or modification stage to incorporate more functional groups, changing its surface chemistry [8]. The aim of the first step usually is to make a carboneous material with initial porosity and functionality, while the second activation/modification step changes the chemical and/or physical properties of the adsorbent to improve its adsorptive removal performance. It has been demonstrated that modification with different acids can enhance the polar functional groups such as carboxylic, phenolic, lactonic, and peroxide on the surface of activated carbon, and improve its hydrophilicity [21, 22]. Chestnut oak shell was selected as carboneous raw material, because, it has hard structure due to the presence of lignin. This characteristic makes it tolerate thermochemical processes without changing into ash. This is of great importance in producing activated carbon adsorbent using natural raw materials. The produced activated carbon from this precursor has the potential to be chemically-modified by simple

modification methods. It is also available and inexpensive in west provinces of Iran.

In this study, the adsorbent was prepared from chestnut oak shell carbonization (and tire waste for comparing the results) followed by modifying with HCl/HNO₃ solution and then used for MB removal from the aqueous solution. Methylene blue is a well-known cationic dye used in the textile industry, biology and medical science [23]. Due to its complex structure, MB is hardly decomposed under natural conditions and thus, it should be removed from wastewaters before releasing to water bodies. The effect of different experimental conditions on the removal efficiency of MB was investigated. The adsorption kinetics and isotherms of MB adsorption and the reusability potential of the adsorbent were also studied.

2. Experimental

2.1. Reagents and materials

All reagents and chemicals were of analytical grade and were prepared from Merck (Darmstadt, Germany). The commercial activated carbon (CAC) was obtained from Cabot Corporation. The MB was obtained from Sigma Aldrich Ltd. (St Louis, USA). The chemical formula of the methylene blue is C₁₆H₁₈ClN₃S*x H₂O (x= 2-3) with the molecular weight of 319.86 g mol⁻¹ (anhydrous), λ_{max} of 664 nm and solubility in water of 50 g L⁻¹. The stock solutions of MB (10000 mg L⁻¹) was prepared by dissolving an appropriate amount of dye in deionized water and working solutions were freshly obtained by appropriate dilution of the MB stock solution.

2.2. Instrumentation

The FTIR spectra were obtained in the range of 400–4000 cm⁻¹ with a Bruker Equinox 55 FTIR spectrometer (Bruker Analytic GmbH, Bremen, Germany). The BET surface area and pore size were obtained from N₂ adsorption-desorption isotherms acquired at 77 K using a Belsorp mini II (BEL Japan Inc., Osaka, Japan). The morphology of the prepared adsorbents was investigated by a TESCAN MIRA III microscope (Czech Republic). The adsorption of the solution was measured through a Specord 200 UV-Vis spectrophotometer (Analytik Jena, Germany).

2.3. Synthesis of activated carbon

Chestnut oak shell activated carbon (CSAC) was prepared according to the procedure below: at first, Chestnut oak shells taken from Zagros forests (Uraman region, Kurdistan, Iran) were thoroughly washed with deionized water and then placed in an oven at 60 °C for 24 h for drying. The dried shells were crushed and powdered using a standard household grinder. In order to carbonization of shells, 50 g of powdered shells were transferred into a stainless steel tube and then placed in an electric furnace at 300 °C under nitrogen atmosphere for 3 h. The rate of heating was set at 5 °C/min. The obtained activated carbon (CSAC) was thoroughly washed with deionized water followed by drying in an oven at 80 °C for 8 h.

The waste rubber-based activated carbon (WRAC) was prepared according to a procedure described in the literature [24]. For this purpose, the waste rubber tire was washed with hot distilled water, dried for 48 h at sunlight and grounded to granules. The material was then heated to 500 °C for 6 h followed by adding hydrogen peroxide (H₂O₂) solution to remove organic impurities. The material was then activated at 900 °C for 2 h under nitrogen atmosphere. After cooling, the obtained residue was rinsed with deionized water and dried.

2.4. Chemical treatment of activated carbon

For acid treatment, 2.0 g of the AC was mixed with the 25 mL of HCl solution (4 M) and stirred on a heater at 60 °C for 6 h. The mixture was then filtered, mixed with 40 mL nitric acid (32.5 %) and heated up to 60 °C for 6 h under stirring with a magnetic stirrer to ensure the complete reaction between the acid and the activated carbon. The resulting product was filtered followed by repeatedly washing with deionized water until reaching a neutral pH (between 6 and 7). Finally, the remaining material was dried in an oven at 100 °C for about 24 h. The obtained acid treated-chestnut shell, waste rubber and commercial activated carbons were labeled as ATCSAC, ATWRAC, and ATCAC, respectively.

2.5. Adsorption experiments

Adsorption experiments were conducted by reacting 0.1 g of adsorbent with 100 mL of MB solution (100 mg L⁻¹) at 25 °C. After adjusting the pH at 7, the

mixture was magnetically stirred with the agitation rate of 200 rpm until the equilibration was achieved. After 20 min, the mixture was filtered and the MB concentration in the residual solution was directly read with the spectrophotometer at the maximum wavelength of 664 nm. All optimization experiments were performed in three replications, and their average values were used as the experimental points in charts. The removal percentage of MB after adsorption by activated carbon was ascribed as follows (Eq. 1):

$$R (\%) = \frac{C_0 - C_t}{C_0} \times 100 \quad (1)$$

Where C₀ and C_t are the initial and remaining MB concentration in the solution at the time 't'. The amount of MB adsorbed on the activated carbon (q_e, mg g⁻¹) was calculated using the equation given below (Eq. 2):

$$q_e = \frac{(C_0 - C_e) \times V}{M} \quad (2)$$

where C_e is the equilibrium MB concentration in the solution (mg L⁻¹), V is the solution volume (L), and M is the mass of the activated carbon (g).

2.6. Adsorption kinetic

Adsorption kinetics was investigated using different models presented in Table 1 (Eqs. 5-8). For this purpose, 0.1 g of the adsorbent was added to a series of aqueous solutions containing 100 mL of 100 mg L⁻¹ MB at the desired temperature and the mixtures were stirred at 200 rpm. The amount of MB adsorbed by the solid phase (q_t, mg L⁻¹) was calculated according to Eq. 3:

$$q_t = \frac{(C_0 - C_t) \times V}{M} \quad (3)$$

2.7. Adsorption isotherms

The equilibrium experiments were performed as follows: 0.1 g of the adsorbent was added to the MB solution (100 mL, pH= 7) with different initial concentrations (C₀ = 50, 100, 150, 200, 250, 300 and 350 mg L⁻¹) and the suspensions were stirred for 24 h at 200 rpm. After reaching the equilibrium, the mixtures were filtered and the concentration of MB in the filtrates was analyzed by the spectrophotometer. The experimental data were fitted to the Langmuir, Freundlich and Temkin isotherm models (Table 1).

Table 1: kinetic and equilibrium equations.

Model	Linear equation	Plots	Parameters
Kinetic models			
Pseudo-first order	$\ln(q_e - q_t) = \ln q_e - k_1 t$ (Eq.5)	$\ln(q_e - q_t)$ vs t	q_t : the adsorption capacity of the adsorbent at any time (mg g^{-1}) q_e : the adsorption capacity of the adsorbent at equilibrium point (mg g^{-1}) k_1 : the pseudo-first-order rate constant (min^{-1}) t : the contact time (min)
Pseudo-second order	$\frac{t}{q_t} = \frac{1}{k_2 \times q_e^2} + \frac{t}{q_e}$ (Eq.6)	t/q_t vs t	k_2 : the pseudo-second-order rate constant ($\text{g mg}^{-1} \text{min}^{-1}$)
Elovich	$q_t = \left(\frac{1}{\beta}\right) \ln \alpha \beta + \left(\frac{1}{\beta}\right) \ln t$ (Eq.7)	q_t vs $\ln(t)$	α : the Elovich initial adsorption rate constant ($\text{mg g}^{-1} \text{min}^{-1}$) β : the Elovich desorption constant (g mg^{-1})
Weber–Morris Intraparticle diffusion	$q_t = k_{id} t^{0.5} + C$ (Eq.8)	q_t vs $t^{0.5}$	k_{id} : the intra-particle diffusion rate constant at any stage “i” ($\text{mg g}^{-1} \text{min}^{-0.5}$) C : is the adsorption rate constant at the stage “i”
Equilibrium models			
Langmuir	$\frac{C_e}{q_e} = \frac{1}{q_m k_L} + \frac{C_e}{q_m}$ (Eq.10)	C_e/q_e vs C_e	C_e : the equilibrium concentration of dye in the solution (mg L^{-1}) q_m : the maximum dye adsorption capacity K_L : the Langmuir constant (L mg^{-1})
Freundlich	$\ln q_e = \frac{1}{n} \ln C_e + \ln k_f$ (Eq.11)	$\ln q_e$ vs $\ln C_e$	K_F : the Freundlich constant (mg g^{-1}) (mg L^{-1}) ^{-1/n} $1/n$: the heterogeneity parameter
Temkin	$q_e = B \ln(A) + B \ln(C_e)$ (Eq.12)	q_e vs $\ln C_e$	C_e : dye concentration (mg L^{-1}) B : Constant related to the heat of sorption (J mol^{-1}) A : Temkin isotherm equilibrium binding constant (L g^{-1})

3. Results and Discussion

3.1. Characterization of the prepared adsorbent

The chemical composition of the adsorbent was studied using FTIR spectroscopy. Figure 1 presented the FTIR spectra of non-modified CSAC and acid-treated activated carbons with similar profiles in their spectra. All spectra showed the characteristic peaks around 3400 cm^{-1} attributed to the O-H stretching vibration of carboxylic acid. The absorption peaks at about 2925 and 2855 cm^{-1} were associated with the C-H vibration. The peaks around 1710 cm^{-1} could be due to the C=O vibration of carboxylic acids, carbonyls, and lactones. The absorption peak at 1621 cm^{-1} showed the presence of C=C of olefins or aromatic rings in the structure. The peaks between 1050 and 1350 cm^{-1} represented the C-O band found in ester, phenol, and ethers. The revealed band at 1700 cm^{-1} is characteristic of the stretching vibration acidic C=O. Also, the amplified and relatively displaced peak (compared to non-modified AC) in $3200\text{-}3700 \text{ cm}^{-1}$ is another sign of acidic surface of modified adsorbent. This peak is related to the stretching vibration of acidic hydroxyl

group.

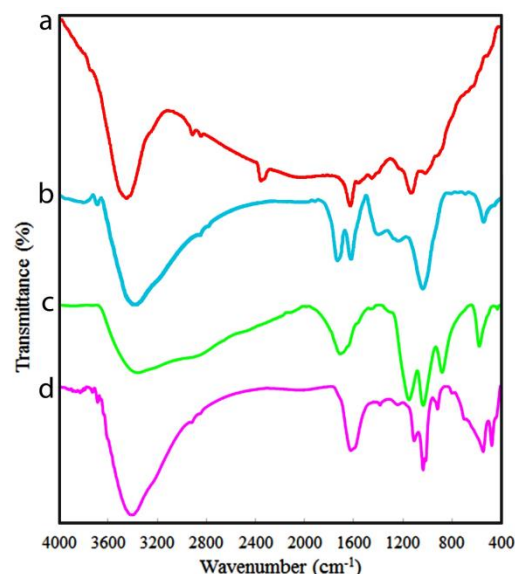


Figure 1: FTIR spectra of (a) chestnut shell, (b) modified chestnut shell AC; (c) modified rubber waste AC; and (d) modified commercial AC.

These bands confirmed the existence of a large amount of oxygen functional groups onto the surface of activated carbons after the acid modification process. The textural parameters of raw and acid-modified activated carbons prepared in this study were presented in Table 1. The results indicated that the prepared materials were porous adsorbent with micro/mesopores. As presented in Table 2, the specific surface area of ATCSAC was found to be $526.53 \text{ m}^2 \text{ g}^{-1}$ which was higher than those of tire activated carbon and commercial activated carbon. This High surface area provides high capacity for dye adsorption. By comparing the S_{BET} of acid treated activated carbons and non-treated AC, it can be seen that S_{BET} is not directly related to the surface area of activated carbons. In some cases, the surface area increases slightly (such as CSAC) and in some cases it causes a decrease in the surface area (such as WRAC and CAC). But in general, acid modification of activated carbons increases the absorption efficiency

due to the change of surface chemistry of the activated carbons.

In accordance with Table 2, the S_{BET} for three adsorbents, are completely different. As can be seen, the removal efficiency of the adsorbents is directly related to S_{BET} . The adsorbent with the highest SBET (ATCSAC, $526.53 \text{ m}^2/\text{g}$) had the highest removal efficiency –based on the experimental results- and it was predictable and reasonable. Indeed, the adsorbent with a high surface area offers more adsorption sites to adsorb the solute molecules.

Figure 2 a-d showed the SEM images of the acid-modified activated carbons. It was obvious that the surface of ATCAC was rough without visible pores. In fact, ATCAC contained channels instead of pores in its structure, given the small surface area from BET analysis. In contrast, the surface of ATCSAC and ATWRAC presented particles with porous structures.

Table 2: The textural parameters obtained from BET analysis and BJH method. S_{BET} : specific surface area, V_t : total pore volume, V_{mic} : micropore volume and D_p : mean pore diameter.

Material	$S_{\text{BET}} (\text{m}^2 \text{ g}^{-1})$	$V_t (\text{m}^3 \text{ g}^{-1})$	$V_{\text{mic}} (\text{m}^3 \text{ g}^{-1})$	$D_p (\text{nm})$
CSAC	520.53	0.3742	0.2360	2.87
ATCSAC	526.53	0.3765	0.2353	5.25
WRAC	90.49	0.3672	0.3618	23.71
ATWRAC	61.934	0.5153	0.4081	28.66
CAC	5.3554	0.016877	0.01500	11.20
ATCAC	2.6144	0.04990	0.04885	28.35

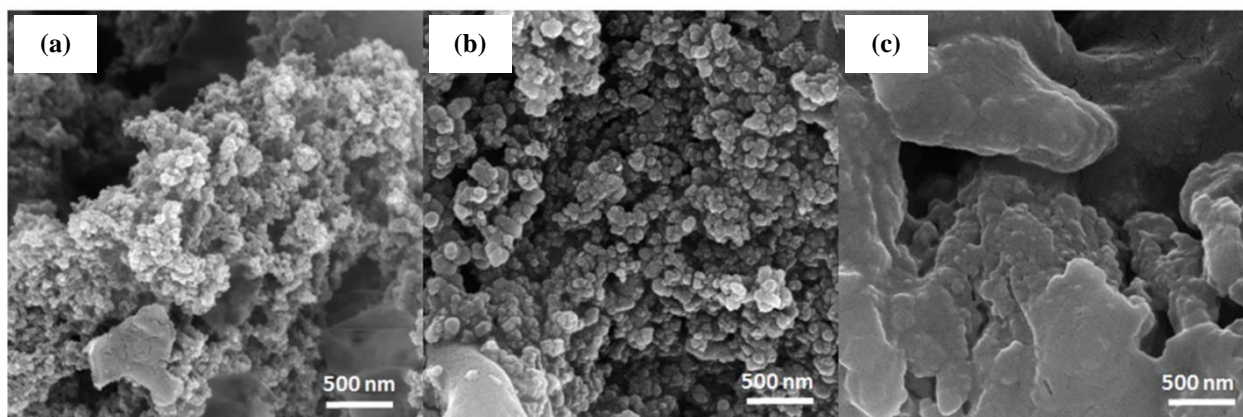


Figure 2: SEM images of (a) modified chestnut shell AC; (b) modified rubber waste AC; and (c) modified commercial AC.

3.2. Chemical treatment of the activated carbon

To investigate the influence of the type and chemical treatment of AC on the dye removal efficiency, the adsorption capacities of the virgin and modified adsorbents were compared with others. The chestnut activated carbon treated with acid showed the best performance for MB adsorption compared to the other adsorbents (Figure 3). Generally, acidic treatment of AC leads to oxidizing its porous structure and changing the surface chemistry of the adsorbent. This, in turn, improves its hydrophilic property. Indeed, oxygen functional groups containing proton donors' are increased on the surface. These functional groups are very effective to interact with positive solutes such as MB in this study. However, acid modification does not significantly change the surface area. The relatively higher surface area and pore volume of chestnut activated carbon, combined with a significant number of polar functional groups created on ATCSAC surface (due to the treatments with HNO₃ and HCl), are significant factors explaining this result [25, 26]. Since the ATCSAC presented the best performance in the primary test, it was selected for the next MB adsorption experiments.

3.3. Optimization of the effective parameters on MB removal

3.3.1. The effect of the pH

The pH of an aqueous solution can change both the surface charge of the adsorbent and the chemical

structure of the analyte. Therefore, the effect of the pH on the MB removal by the adsorbent was studied by varying the pH in the range of 3-11. For this purpose, 0.1 g of the ATCSAC was added to a series of MB solutions (100 mL, 100 mgL⁻¹) and the pH was fixed at the desired value by adding an appropriate amount of HNO₃ or NaOH solution. Then, the MB concentration was measured on the remaining solutions after 10 min stirring (with 200 rpm). As shown in Figure 4a, the MB removal percentages were almost constant and slight enhancement in the removal percentage was observed by increasing the pH of the solution. It can be suggested that both electrostatic and non-electrostatic interactions involved in the dye adsorption process. At pH values higher than the pK_a (~ 3.8) of the dye and the pH_{pzc} (3.2) of the adsorbent, the attractive force between the negatively charged AAC and positively charged MB favored the dye adsorption. Therefore, increasing the solution pH can enhance the adsorption capacity of the dye. On the other hand, MB is an electron donor molecule due to the existence of benzene rings and heteroatoms (N and S) in its chemical structure. Thus, besides the electrostatic forces, MB can be adsorbed on the surface of ATCSAC via non-electrostatic interactions such as π - π stacking, hydrogen bonding and hydrophobic forces which caused a little impact on the dye adsorption capacity by changing the sample solution pH. Since the removal efficiencies were almost constant in the pH range of 5 to 11, a fixed pH of 7 was selected in this study.

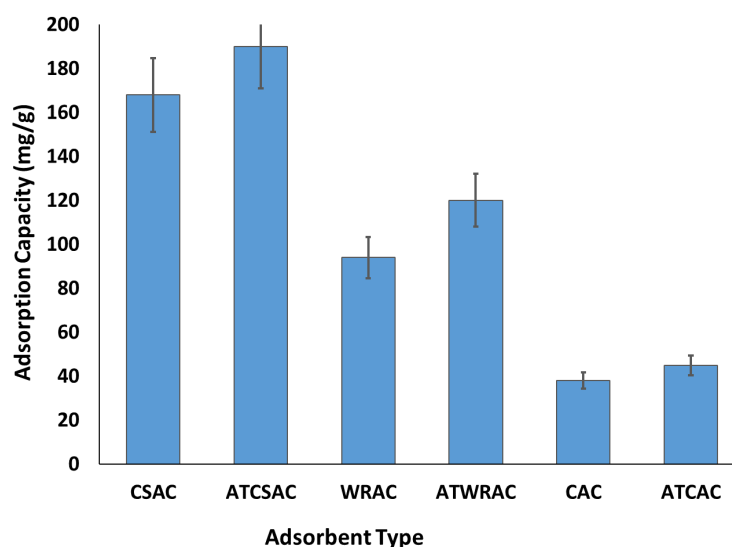


Figure 3: Comparison of the MB adsorption capacity of virgin and acid treated activated carbons prepared in this study.

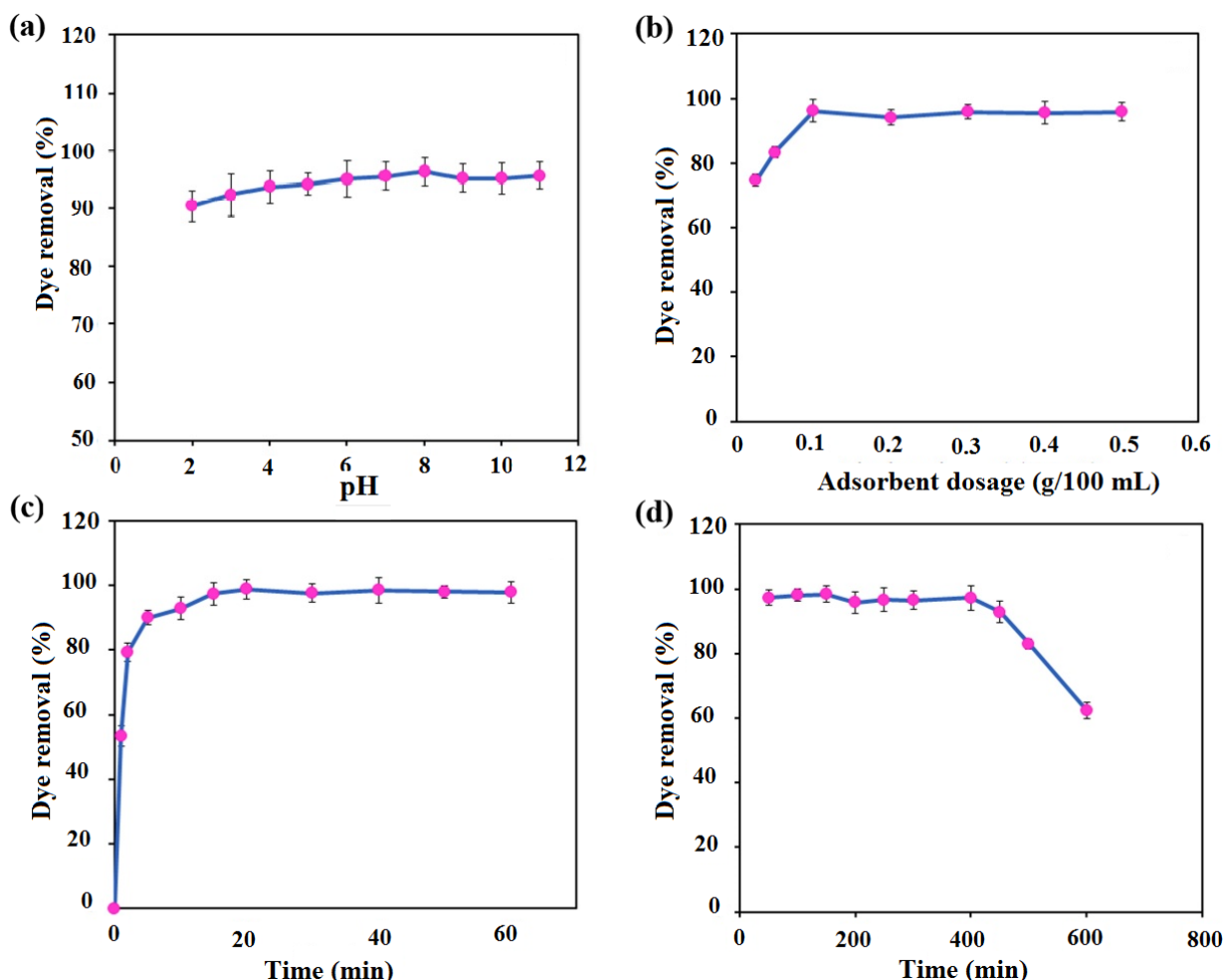


Figure 4: The effect of (a)pH;(b) adsorbent dosage; (c) contact time; and (d) initial dye concentration on the MB removal efficiency.

3.3.2. Effect of adsorbent dosage

It has been shown that the removal efficiency of analytes is strongly affected by the mass of the adsorbent. The insufficient amount of the adsorbent, cannot provide enough active sites for complete adsorption of the analyte while the excessive usage of the adsorbent increases the operating costs in practical applications. Therefore, the adsorbent loading should be optimized during an adsorption process. In this study, the effect of adsorbent dosage on the MB removal efficiency was investigated in the range of 0.025 to 0.5 g and the experimental results were presented in Figure 4b. The MB removal was highly dependent on the adsorbent dosage and increasing of the adsorbent loading from 0.025 to 0.1 g enhanced the MB removal percentage. The higher amount of the adsorbent increased the available active sites for the adsorption of MB molecules. Further Increasing the adsorbent dosage to 0.5 g showed almost constant

removal efficiencies. Hence, the optimum amount of 0.1 g of the adsorbent was selected for the next experiments.

3.3.3. Effect of contact time

Since the adsorption is an equilibrium process, it is essential to allow the adsorbent to contact with the dye molecules sufficiently. Analytes cannot reach its equilibrium over insufficient contact times while excessive contact times can increase the whole analysis time and operational cost. Due to the importance of this issue, the influence of contact time on the MB removal efficiency using ATCSAC was analyzed at 100 mg L⁻¹ of initial MB concentration, 0.1 g of the adsorbent and contact times varying from 1 to 60 min. The results (Figure 4c) showed a sharp increase in the MB removal efficiency within the first 5 min of the contact time (with the dye removal up to 90.1 %), continued by a gradual enhancement in the removal efficiency until

the adsorption equilibrium was achieved at 20 min (with the dye removal of 98.9 %). After the equilibrium point, no significant change was observed in the removal efficiency of MB by extending the contact time up to 60 min due to the saturation of all active sites by MB molecules indicating that sorption equilibrium was achieved at 20 min. Numerous active sites on the adsorbent surface are easily available in the initial stage of the adsorption process, thus the adsorption occurred faster caused a sharp increase in the amounts removed. When the easy-accessed active sites of the adsorbent were occupied by MB molecules, the rate of adsorption is decreased and reached nearly constant at equilibrium. Finally, the time of 20 min was chosen to ensure attaining the adsorption equilibrium.

3.3.4. Effect of initial MB concentration

Although the dye concentration level in effluents of dye-related factories is varied and depends on different factors, the influence of initial dye concentration on the removal efficiency was investigated at different concentration levels in the range of 50 to 600 mg L⁻¹ under optimized other conditions. The results were illustrated in Figure 4d. It was observed that the removal percentages were almost constant by increasing the initial MB concentration from 50 to 400 mg L⁻¹. However, by further increasing the initial concentration of the MB solution from 400 mg L⁻¹ to 600 mg L⁻¹, the dye removal percentage decreased from 97.2 to 62.4 % due to the saturation of all active adsorption sites. At very high concentrations, the number of binding sites is not sufficient to adsorb all MB molecules leading to the decrease of dye removal percentages.

3.4. Adsorption kinetics

The adsorption capacity of MB on ATCSAC was investigated as a function of time between 0 to 60 min (Figure 5a). As obvious, the adsorption rate was rapid in the first 5 min of the removal process, after that the rate of adsorption slowed down until reached equilibrium at about 20 min. In order to study the MB adsorption mechanism on the ATCSAC, common kinetic models including the pseudo-first-order, pseudo-second-order, Elovich, and intraparticle diffusion models were used to fit the experimental data (Table 1). The linearized kinetic models fitted with the experimental results were shown in Figure 5b-e and the parameters corresponding to each

model were summarized in Table 3. The results ($R^2 > 0.9$) suggested a well-fitting of all models with the experimental data when the pseudo-second-order kinetic ($R^2 = 0.9996$) showed better fit to the adsorption kinetic data compared to the other models. The kinetics of adsorption was also investigated by fitting the data to the Weber and Morris model. As shown in Figure 5e, the plot of q_t versus $t^{0.5}$ did not pass through the origin indicating that the adsorption mechanism of MB is not controlled by intra-particle diffusion. The fit of data showed three successive steps: the first step with a fast uptake rate at the first 5 min of the adsorption process suggesting the fast external diffusion of MB through the solution to the adsorbent surface, the next step (5–20 min) with a gradual adsorption rate which was due to the MB migration from the external surface into the ATCSAC pores and adsorption to the inner active sites and the final step (20–60 min) where the adsorption reached its equilibrium, and most of available active sites on the ATCSAC surface were occupied by MB molecules.

3.5. Adsorption equilibrium isotherms

In the present study, the Langmuir, Freundlich and Temkin isotherms were selected to investigate the MB adsorption process on ATCSAC (Table 1). The related isotherm parameters determined from the corresponding linear fitting were summarized in Table 4. The linear plots of these equilibrium models were also shown in Figure 6. According to the results (R^2 values) obtained from three isotherms investigated in this work, best linearity was obtained by fitting the data with the Freundlich model indicating the multilayer adsorption of MB dye on the various binding active sites of the ATCSAC. The Freundlich parameter $1/n = 0.8063$ obtained from the slope of the Freundlich linear plot (Figure 6b and Table 4) fallen between 0 and 1 suggesting a linear and uniform adsorption throughout the adsorbent surface [27]. In addition, the value of n can indicate the favorability of the adsorption mechanism. Adsorption is favorable when the value of n is greater than one [3]. In this study, the value of “ n ” found to be 1.24 which was greater than one confirming the favorability of the adsorption. This result was in agreement with other studies in the literature [28, 29]. The maximum sorption capacity of the adsorbent using the Langmuir model was obtained to be 406.21 mg g⁻¹ at 25 °C.

Table 3: Parameters of different kinetic models obtained for MB adsorption.

Model	Parameters	Value
Pseudo first order	q_e (mg g ⁻¹)	331.307
	K_1 (min ⁻¹)	0.1457
	R^2	0.9904
Pseudo second order	q_e (mg g ⁻¹)	401.34
	K_2 (g mg ⁻¹ min ⁻¹)	0.00084
	R^2	0.9996
Elovich	α	346.703
	β	0.01314
	R^2	0.9852
Intraparticle diffusion	$C_{i,1}$	-2.0373
	$k_{i,1}$ (mg g ⁻¹ min ^{-0.5})	113.6
	R^2	0.9918
	$C_{i,2}$	180.27
	$k_{i,2}$ (mg g ⁻¹ min ^{-0.5})	38.209
	R^2	0.9964
	$C_{i,3}$	358
	$k_{i,3}$ (mg g ⁻¹ min ^{-0.5})	2.602
	R^2	0.9115
	C_i	83.278
	k_i (mg g ⁻¹ min ^{-0.5})	51.125
	R^2	0.847

Table 4: The parameters of adsorption isotherms obtained for MB adsorption onto the ATCSAC.

Model	Parameters	Value
Langmuir	q_m (mg g ⁻¹)	406.2117
	K_L (L mg ⁻¹)	0.03221
	R^2	0.9867
Freundlich	1/n	0.8063
	K_F (mg g ⁻¹) (mg L ⁻¹) ^{-1/n}	14.8759
	R^2	0.997
Temkin	A_T (L g ⁻¹)	0.6181
	B	58.829
	R^2	0.9503

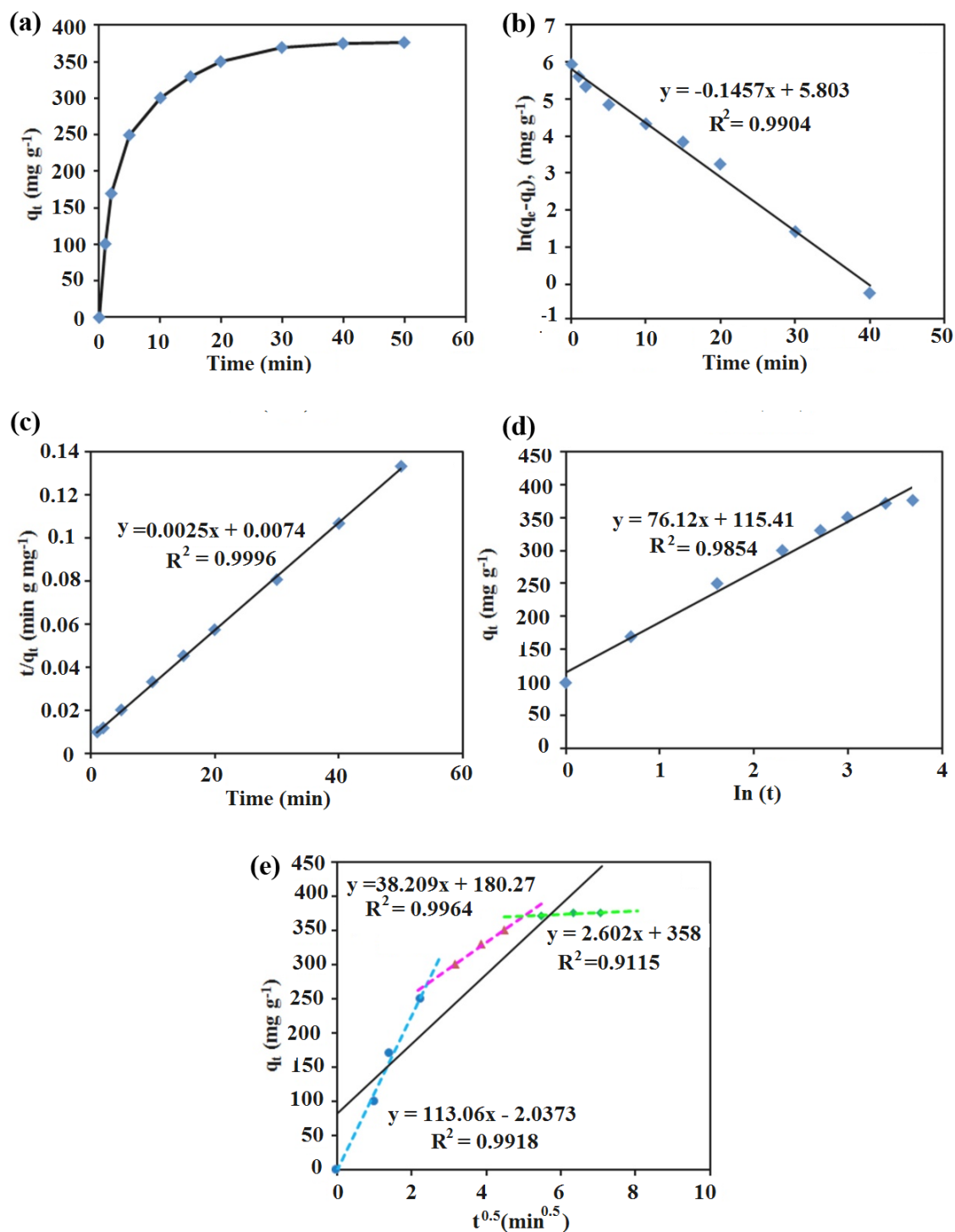


Figure 5: (a) The linear plots of MB adsorption models: (b) pseudo first order model, (c) pseudo second order model, (d) Elovich model, (e) Weber Morris intra-particle diffusion model.

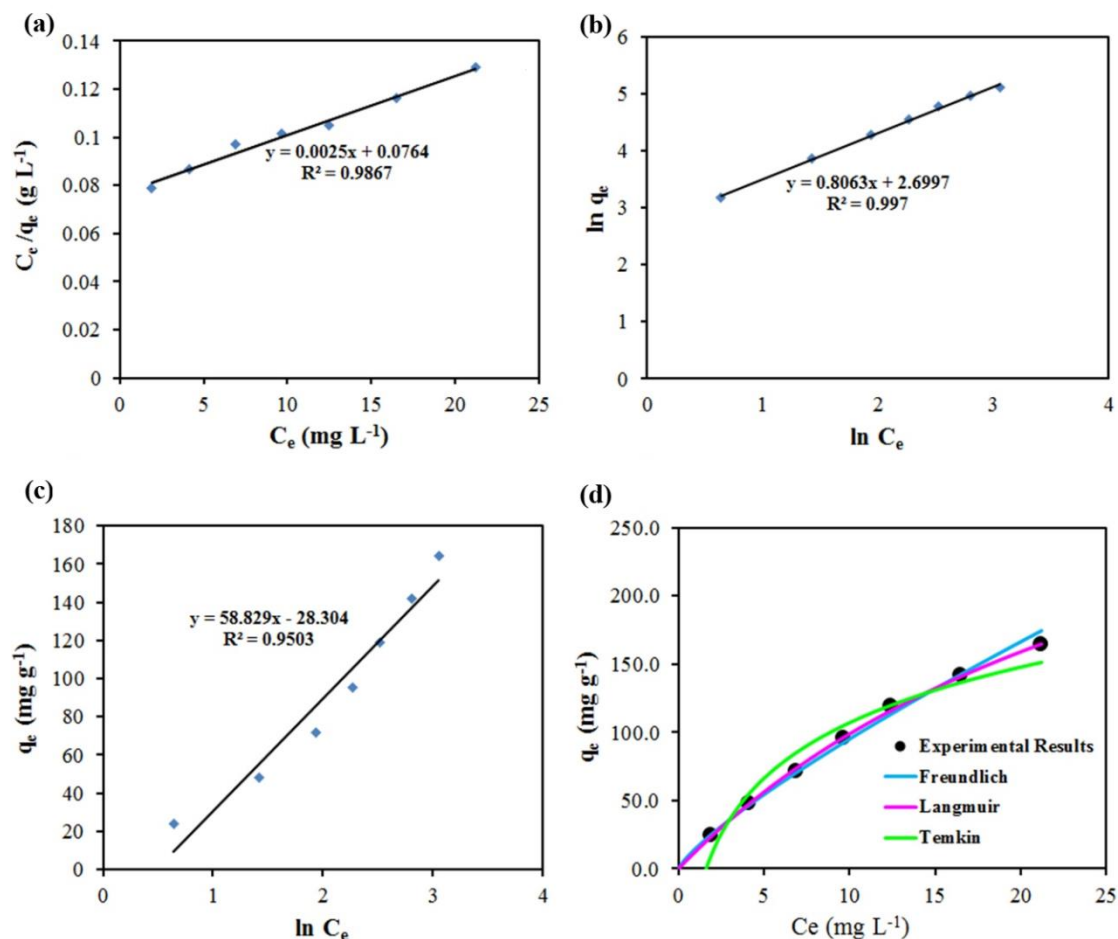


Figure 6: The linear plots of MB equilibrium isotherms (a) Langmuir model, (b) Freundlich model, and (c) Temkin model. (d) equilibrium isotherms of MB adsorption on ATCSAC.

Table 5: The results of BJH.

The experiment	Results of the oak	Acidic modification	Basic modification
Plot data	Adsorption branch	Adsorption branch	Adsorption branch
V_p [$\text{cm}^3 \text{g}^{-1}$]	0.2353	0.2353	0.5102
rp,peak(Area)	1.21	1.29	1.29
A_p [$\text{m}^2 \text{g}^{-1}$]	211.92	211.92	340.95

3.6. Comparison with other adsorbents

The adsorption capacity of ATCSAC was compared to those obtained from different activated carbons toward the MB adsorption. As can be seen from the results summarized in Table 5, the ATCSAC had higher adsorption capacity than many of activated carbons for MB adsorption indicating the great potential of ATCSAC as a low-cost adsorbent for use in water and wastewater treatment processes. The high adsorption ability of the prepared adsorbent may be ascribed to the

porous structure and the presence of various oxygen-functional groups on the surface of AC created by acid treatment leading to a variety of interactions with MB molecules such as electrostatic attraction, π - π interaction and hydrogen bonding.

3.7. Reusability of the adsorbent

The reusability of adsorbents is an important issue for reducing the overall cost in practical applications. The reusability of the adsorbent was studied by the

successive adsorption/desorption cycle of MB onto the ATCSAC for ten times. For this purpose, after completing the adsorption process, the spent adsorbent was washed with a methanol solution containing 5 % (v/v) NaOH to recover the MB adsorbed on ATCSAC. Next, the adsorbent was thoroughly washed with deionized water and subjected to the next adsorption experiment according to the procedure described in Section 2.5. As shown in Figure 7, the adsorption capacity of the ATCSAC remained 95.5 % of its initial capacity after ten regeneration cycles with a removal efficiency higher than 92.7 %, indicating a good regenerability of the adsorbent. Therefore, the ATCSAC can serve as a potential adsorbent for removing MB dye in water treatment based on an economic viewpoint.

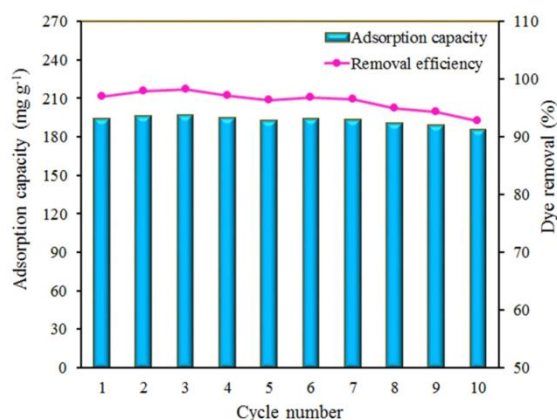


Figure 7: Reusability of the prepared ATCSAC adsorbent for different cycles.

4. Concluding

In this study, an acid modified-AC prepared from the chestnut oak shell (ATCSAC) was prepared and its adsorptive performance was used for MB removal from aqueous solution. Besides the high BET surface area of the ATCSAC ($526 \text{ m}^2 \text{ g}^{-1}$) and its porous structure, creation large amounts of oxygen functional groups due to the modification with acid provided numerous binding sites to adsorb dye molecules. The optimal operating parameters for obtaining the maximum adsorption capacity and highest removal efficiency were found to be: pH between 5 and 11, the adsorbent dosage of 0.1 g in 100 mL, the contact time of 20 min and initial dye concentration of 50-400 mg L^{-1} . The kinetics of sorption was found to follow the pseudo-second-order model. Meanwhile, the equilibrium data were fitted well with the Freundlich isotherm models which confirmed that the sorption is heterogeneous and occurred via physic-chemical interactions. Moreover, the adsorbent showed high adsorption capacity (406.21 mg g^{-1}) for MB which was better than those of several ACs reported in the literature. The regeneration experiments indicated that the prepared ATCSAC had good reusability at least for ten cycles. These results indicated that the ATCSAC can be applied as a low cost and efficient adsorbent for dye removal from aqueous media.

5. References

- Shittu, A. Achazhiyath Edathil, A. Alsaeedi, S. Al-Asheh, K. Polychronopoulou, F. Banat, Development of novel surfactant functionalized porous graphitic carbon as an efficient adsorbent for the removal of methylene blue dye from aqueous solutions, *J. Water Process Eng.*, 28(2019), 69-81.
- D. Kanakaraju, N. R. Mohamad Shahdad, Y. C. Lim, A. Pace, Magnetic hybrid $\text{TiO}_2/\text{Alg}/\text{FeNPs}$ triads for the efficient removal of methylene blue from water, *Sustain. Chem. Pharm.*, 8(2018), 50-62.
- P. Nautiyal, K. A. Subramanian, M. G. Dastidar, Adsorptive removal of dye using biochar derived from residual algae after in-situ transesterification: Alternate use of waste of biodiesel industry, *J. Environ. Manage.*, 182(2016), 187-197.
- I. Khan, M. Sadiq, I. Khan, K. Saeed, Manganese dioxide nanoparticles/activated carbon composite as efficient UV and visible-light photocatalyst, *Environ. Sci. Pollut. Res.*, 26(2019), 5140-5154.
- L. Ai, C. Zhang, F. Liao, Y. Wang, M. Li, L. Meng, J. Jiang, Removal of methylene blue from aqueous solution with magnetite loaded multi-wall carbon nanotube : Kinetic , isotherm and mechanism analysis, *J. Hazard. Mater.*, 198(2011), 282-290.
- S. Y. Gu, C. Te Hsieh, Y. A. Gandomi, Z. F. Yang, L. Li, C.C. Fu, R.S. Juang, Functionalization of activated carbons with magnetic Iron oxide nanoparticles for removal of copper ions from aqueous solution, *J. Mol. Liq.*, 277(2019), 499-505.
- A. Nasrullah, A. H. Bhat, A. Naeem, M. H. Isa, M. Danish, High surface area mesoporous activated

- carbon-alginate beads for efficient removal of methylene blue, *Int. J. Biol. Macromol.*, 107(2018), 1792-1799.
8. F. Alakhras, I. Anastopoulos, E. C. Lima, E. I. Unuabonah, A. Meknati, S. A. Sajjadi, A. Hosseini-Bandegharai, D. I. Mendoza-Castillo, P. Singh, G. L. Dotto, A novel route for preparation of chemically activated carbon from pistachio wood for highly efficient Pb(II) sorption, *J. Environ. Manage.*, 236(2019), 34-44.
 9. S. K. Theydan, M. J. Ahmed, Adsorption of methylene blue onto biomass-based activated carbon by FeCl₃ activation: Equilibrium, kinetics, and thermodynamic studies, *J. Anal. Appl. Pyrolysis.*, 97(2012), 116-122.
 10. E. Bibaj, K. Lysigaki, J. W. Nolan, M. Seyedsalehi, E. A. Deliyanni, A. C. Mitropoulos, G. Z. Kyzas, Activated carbons from banana peels for the removal of nickel ions, *Int. J. Environ. Sci. Technol.*, 16(2019), 667-680.
 11. M. K. B. Grauto, T. Panyathanmaporn, R. A. Chumnanklang, N. Sirinuntawittaya, A. Dutta, Production of activated carbon from coconut shell: Optimization using response surface methodology, *Bioresour. Technol.*, 11(2008) 4887-4895.
 12. F. Cao, C. Lian, J. Yu, H. Yang, S. Lin, Study on the adsorption performance and competitive mechanism for heavy metal contaminants removal using novel multi-pore activated carbons derived from recyclable long-root *Eichhornia crassipes*, *Bioresour. Technol.*, (2019), 211-218.
 13. N. Boudechiche, M. Fares, S. Ouyahia, H. Yazid, M. Trari, Z. Sadaoui, Comparative study on removal of two basic dyes in aqueous medium by adsorption using activated carbon from *Ziziphus lotus* stones, *Microchem. J.*, 146(2019) 1010-1018.
 14. D. Garg, S. Kumar, K. Sharma, C. B. Majumder, Application of waste peanut shells to form activated carbon and its utilization for the removal of Acid Yellow 36 from wastewater, *Grandwater Sustain Develop.*, 8(2019), 512-519.
 15. R. Lafi, I. Montasser, A. Hafiane, Adsorption of congo red dye from aqueous solutions by prepared activated carbon with oxygen-containing functional groups and its regeneration, *Adsorpt. Sci. Technol.*, 37(2019), 160-181.
 16. M. Ziati, S. Hazourli, Experimental investigation of activated carbon prepared from date stones adsorbent electrode for electrosorption of lead from aqueous solution, *Microchem. J.*, 14 (2019), 164-169.
 17. V. K. Gupta, B. Gupta, A. Rastogi, S. Agarwal, A. Nayak, Pesticides removal from waste water by activated carbon prepared from waste rubber tire, *Water Res.*, 45(2011), 4047-4055.
 18. V. K. Gupta, A. Nayak, S. Agarwal, I. Tyagi, Potential of activated carbon from waste rubber tire for the adsorption of phenolics: Effect of pre-treatment conditions, *J. Colloid Interface Sci.*, 417(2014), 420-430.
 19. B. Ebrahimi, S. Mohammadiazar, S. Ardalani, New modified carbon based solid phase extraction sorbent prepared from wild cherry stone as natural raw material for the pre-concentration and determination of trace amounts of copper in food samples, *Microchim. J.*, 147(2019), 666-673.
 20. J. Wang, J. Zhang, L. Yue, Y. Qin, L. Shi, H. Wu, H. Du, R. Chen, Synthesis of activated carbon from peanut shell as dye adsorbents for wastewater treatment, *Adsorpt. Sci. Technol.*, 37(2019), 34-48.
 21. M. E. de Oliveira Ferreira, B. G. Vaz, C. E. Borba, C. G. Alonso, I. C. Ostroski, Modified activated carbon as a promising adsorbent for quinoline removal, *Microporous Mesoporous Mater.*, 277(2019), 208-216.
 22. S. Karagöz, T. Tay, S. Ucar, M. Erdem, Activated carbons from waste biomass by sulfuric acid activation and their use on methylene blue adsorption, *Bioresour. Technol.*, 99(2008), 6214-6222.
 23. D. Pathania, S. Sharma, P. Singh, Removal of methylene blue by adsorption onto activated carbon developed from *Ficus carica* bast, *Arab. J. Chem.*, 10(2017), S1445-S1451.
 24. V. K. Gupta, I. Ali, T. A. Saleh, M. N. Siddiqui, S. Agarwal, Chromium removal from water by activated carbon developed from waste rubber tires, *Environ. Sci. Pollut. Res.*, 20(2013), 1261-1268.
 25. M. Laabd, Y. Brahmi, B. El Ibrahim, A. Hsini, E. Toufik, Y. Abdellaoui, H. Abou Oualid, M. El Ouardi, A. Albourine, A novel mesoporous Hydroxyapatite@Montmorillonite hybrid composite for high-performance removal of emerging Ciprofloxacin antibiotic from water: Integrated experimental and Monte Carlo computational assessment, *J. Mol. Liq.*, 338(2021), 116705-116720.
 26. Y. Abdellaoui, B. El Ibrahim, H. Abou Oualid, Z. Kassab, C. Quintal-Franco, G. Giacomani-Vallejos, P. Gamero-Melo, Iron-zirconium microwave-assisted modification of small-pore zeolite W and its alginate composites for enhanced aqueous removal of As(V) ions: Experimental and theoretical studies, *Chem. Eng. J.*, 421(2021), 129909-129925.
 27. A. L. Ahmad, M. M. Loh, J. A. Aziz, Preparation and characterization of activated carbon from oil palm wood and its evaluation on Methylene blue adsorption, *Dye. Pigm.*, 75(2007), 263-272.
 28. Y. C. Sharma, Uma, Optimization of parameters for adsorption of methylene blue on a low-cost activated carbon, *J. Chem. Eng. Data.*, 55(2010), 435-439.
 29. Y. Li, Q. Du, T. Liu, X. Peng, J. Wang, J. Sun, Y. Wang, S. Wu, Z. Wang, Y. Xia, L. Xia, Comparative study of methylene blue dye adsorption onto activated carbon, graphene oxide, and carbon nanotubes, *Chem. Eng. Res. Des.*, 91(2013), 361-368.
 30. A. A. Attia, B. S. Girgis, N. A. Fathy, Removal of methylene blue by carbons derived from peach stones by H₃PO₄ activation: Batch and column studies, *Dye. Pigm.*, 76(2008), 282-289.

31. B. H. Hameed, A. L. Ahmad, K. N. A. Latiff, Adsorption of basic dye (methylene blue) onto activated carbon prepared from rattan sawdust, *Dye. Pigm.*, 75(2007), 143-149.
32. A. Islam, M. J. Ahmed, W. A. Khanday, M. Asif, B. H. Hameed, Mesoporous activated carbon prepared from NaOH activation of rattan (*Lacosperma secundiflorum*) hydrochar for methylene blue removal, *Ecotoxicol. Environ. Saf.*, 138(2017), 279-285.
33. E. Altıntig, H. Altundag, M. Tuzen, A. Sari, A. Sari, Effective removal of methylene blue from aqueous solutions using magnetic loaded activated carbon as novel adsorbent, *Chem. Eng. Res. Des.*, 122(2017), 151-163.
34. M. A. Islam, S. Sabar, A. Benhouria, W. A. Khanday, M. Asif, B. H. Hameed, Nanoporous activated carbon prepared from karanj (*Pongamia pinnata*) fruit hulls for methylene blue adsorption, *J. Taiwan Inst. Chem. Eng.*, 74(2017), 96-104.

How to cite this article:

F. Shirzadi, B. Ebrahimi, A. Roostaie, S. Mohammadiazar, Acid Modified Activated Carbon Derived from Chestnut Oak Shells for Adsorption and Removal of Methylene Blue from Aqueous Solution. *J. Prog. Color Colorants Coat.*, 16 (2023), 139-152.

